AIP Applied Physics Letters

Metallic percolation in La 0.67 Ca 0.33 MnO 3 thin films

S. F. Chen, P. I. Lin, J. Y. Juang, T. M. Uen, K. H. Wu, Y. S. Gou, and J. Y. Lin

Citation: Applied Physics Letters **82**, 1242 (2003); doi: 10.1063/1.1554768
View online: http://dx.doi.org/10.1063/1.1554768
View Table of Contents: http://scitation.aip.org/content/aip/journal/apl/82/8?ver=pdfcov
Published by the AIP Publishing

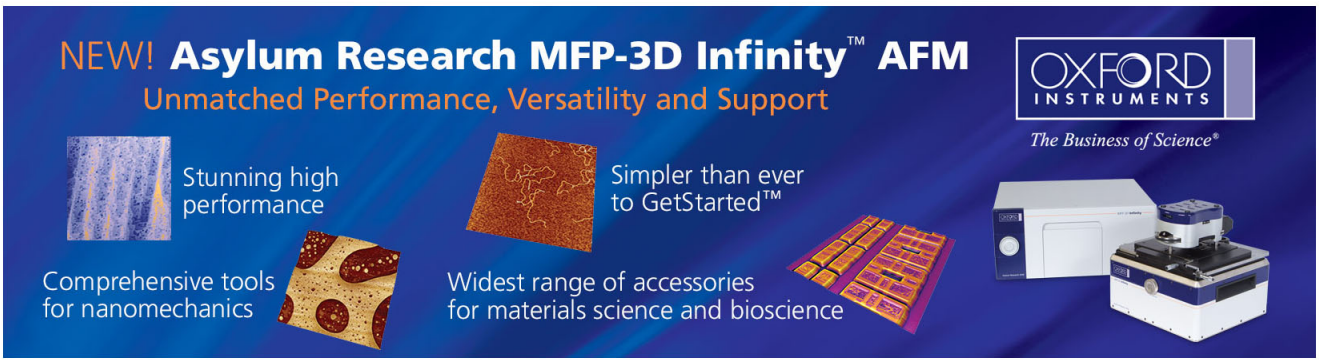

Metallic percolation in $La_{0.67}Ca_{0.33}MnO_3$ thin films

S. F. Chen,[a] P. I. Lin, J. Y. Juang, T. M. Uen, K. H. Wu, and Y. S. Gou
Department of Electrophysics, National Chiao Tung University, Hsinchu 300, Taiwan

J. Y. Lin
Institute of Physics, National Chiao Tung University, Hsinchu 300, Taiwan

(Received 3 September 2002; accepted 31 December 2002)

Phase separation in $La_{0.67}Ca_{0.33}MnO_3$ thin films was investigated by scanning tunneling microscopy. The correlation between the grain structure and the spatial distribution of the coexisting metallic and insulating phases was evidently established. At temperatures not far below the metal–insulator transition, the spatial variation of the coexisting metallic and insulating phases is susceptible to magnetic field in an irreversible manner. The irreversibility suggests that the metallic percolation paths can be affected randomly by magnetic field. However, the variation becomes insensitive to magnetic field at lower temperatures. © *2003 American Institute of Physics.*
[DOI: 10.1063/1.1554768]

Recently, the doped rare-earth manganites ($R_{1-x}A_xMnO_3$ with R being a trivalent rare-earth ion and A being a divalent dopant) have become the focus of attention owing to the colossal magnetoresistance (CMR) and a wealth of phase states exhibited in this class of materials.[1] The undoped $LaMnO_3$, for example, is an antiferromagnetic insulator over all temperature ranges. Partial substitution of La ions with divalent alkali earth ions, however, leads to a ferromagnetic metal transition at an ordering temperature T_C. For $La_{1-x}Ca_xMnO_3$, this ferromagnetic transition is usually accompanied by a metal–insulator transition (MIT) in the nominal range of $0.2<x<0.5$. The transition temperature is approximately 250 K for $x=0.375$. The double exchange mechanism, describing the hopping of electrons between Mn^{3+} and Mn^{4+} sites through O^{2-} ions, qualitatively explains the coincidence of metallic behavior and ferromagnetic ordering commonly observed in CMR materials.[2] It has been pointed out, however, that the double exchange mechanism alone is insufficient to explain the high-temperature transport properties of most manganites.[3,4]

Recent studies, moreover, have revealed that CMR is intimately associated with spatial inhomogeneity of charge and is suggestive of multiphase coexistence.[5] In order to understand the transport properties of manganites, scanning tunneling microscopy (STM) has been ubiquitously adopted to probe the electronic properties of manganites.[6–11] Fäth *et al.*[10] have utilized STM spectroscopic images taken just below T_C to demonstrate the coexistence of insulating and metallic phases in $La_{0.7}Ca_{0.3}MnO_3$ thin films. In addition, by observing the spatial variations of phase separation modulated by magnetic fields, the authors have proposed that the MIT and the magnetoresistance are originated from the percolated metallic ferromagnetic domains. On the other hand, Grévin *et al.*[11] have utilized a technique of scanning tunneling potentiometry to measure the potential distribution at the surface of $La_{0.7}Sr_{0.3}MnO_3$ thin films. Even though the results support the general idea of percolation paths, the nature of percolation paths, however, is claimed to be different from that proposed by Fäth *et al.*[10] In the latter case, grain boundaries, which characterize the connection of adjacent grains, are the key to determine the low resistance percolation paths. We noted that the discrepancy may be due to different materials being studied.

In this study, the local electronic properties affected by a magnetic field in $La_{0.67}Ca_{0.33}MnO_3$ thin films were investigated by STM. At temperatures below T_C, phase separation was observed. Near T_C, the spatial variation of the separated phases is susceptible to the external magnetic field in an irreversible manner. Moreover, the distribution of coexisting phases and, hence, the percolation paths, appears to be correlated with the grain structure in $La_{0.67}Ca_{0.33}MnO_3$ thin films.

$La_{0.67}Ca_{0.33}MnO_3$ samples were grown on single crystal (100) $SrTiO_3$ substrates using pulsed laser deposition. The substrate temperature was held at 700 °C and oxygen pressure was kept at 0.4 Torr during deposition. After deposition was completed, the samples were annealed *in situ* at the same temperature in 600 Torr of pure oxygen for 30 min and then cooled down to room temperature at a cooling rate of 15 °C/min. The film thickness was estimated to be approximately 300 nm from the number of laser pulses delivered. The resistance peak temperature denoted as metal-insulator transition (T_{MI}) is 260 K. The Curie temperature of $La_{1-x}Ca_xMnO_3$ thin films has been found to coincide with T_{MI} within 10 K.[12,13] The x-ray diffraction results showing only $(00l)$ peaks confirm that the samples were epitaxially grown with well-aligned crystalline orientation.

The surface topographic and spectroscopic images were measured by STM operated at constant-current mode with a metallic $Pt_{0.8}$:$Ir_{0.2}$ tip. The tunneling current was set to 500 pA and the sample was biased at 0.3 V relative to tip potential. A standard lock-in technique was used for the measurement of spectroscopic images. All images were measured at a very slow scanning rate by recording both the z-axis signal of the piezoscanner and the differential conductance ($dI/dV|_{0.3\ V}$) signal from the lock-in amplifier. The lock-in amplifier sensed the modulated tunneling current signal and

[a]Electronic mail: sfchen.ep86g@nctu.edu.tw

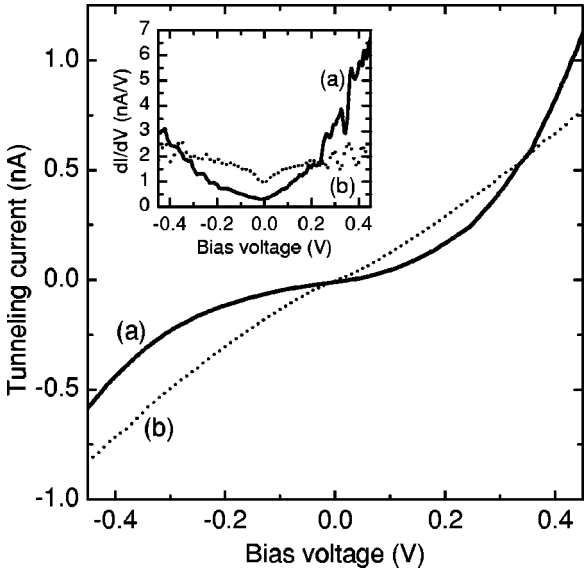

FIG. 1. Typical current–voltage characteristics of (a) insulating phase and (b) metallic phase. The inset shows the differential tunneling spectra (dI/dV) obtained from the respective current–voltage characteristics.

generated dI/dV signal simultaneously to form spatial spectroscopic images during scanning.

Figure 1 shows the tunneling spectra obtained by recording the tunneling current as a function of bias voltage with the feedback loop turned off. The inset shows the dI/dV curves obtained from the tunneling spectra. The highly nonlinear current–voltage characteristic [curve (a)] reflects the signature of an insulating state whereas the nearly linear current–voltage characteristic [curve (b)] depicts a metallic behavior. The difference in $dI/dV|_{0.3V}$ forming the spatial spectroscopic images thus reveals the insulating and metallic phase distribution over the scanning area.

In Fig. 2, the topographic and spectroscopic images are

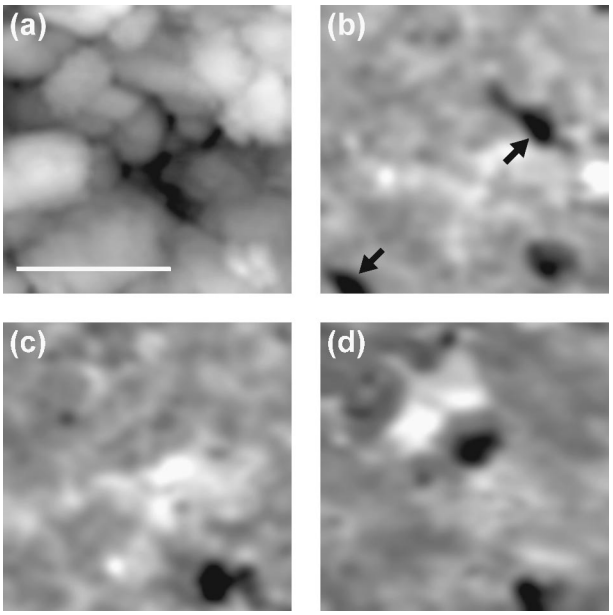

FIG. 2. (a) The zero-field topographic image at 200 K. The scale bar is 40 nm. (b) to (d) are spectroscopic images taken over the same scanning region, with (b) at initial zero field, (c) in an external magnetic field of 0.35 T and (d) after removal of the external magnetic field, respectively. The arrows in (b) indicate regions with metallic characteristic.

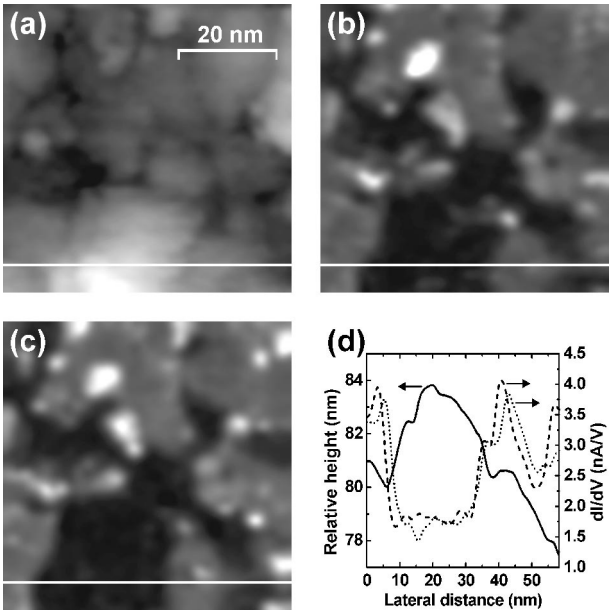

FIG. 3. (a) The topographic image at 100 K. (b) and (c) are spectroscopic images taken over the same scanning region with zero and an external magnetic field of 0.35 T, respectively. (d) The sectional curves scanned along the white lines in the images of surface topography (solid curve) and spectroscopic images at $H=0$ T (dotted curve) and $H=0.35$ T (dashed curve), respectively. The results indicate intimate correlation between the grain structure and the corresponding phases.

illustrated for the same scanning region taken at a temperature (200 K) not far below $T_{MI}(\sim 260\,\mathrm{K})$. The lighter gray regions in the spectroscopic images represent regions with higher dI/dV and, hence, are more insulating. By the same token, the darker regions are more metallic. It is noted, however, that the gray scale in each image is displayed in the highest contrast and does not correspond to the same dI/dV value. Figure 2(a) shows a surface topographic image over the same region the other spectroscopic images were measured. As can be seen, when no external magnetic field was applied, most of the area [Fig. 2(b)] exhibits insulating phase with a small fraction of metallic regions. When an external field of 0.35 T was applied parallel to the film surface, the distribution of the respective phases changes dramatically [Fig. 2(c)]. For instance, two of the metallic regions [indicated by the arrows in Fig. 2(b)] appear to convert into insulating state. When the external field was removed, the spectroscopic image, shown in Fig. 2(d), surprisingly does not recover to that shown in Fig. 2(b). It appears that the phase distribution is irreversible and is dependent on the history of the applied magnetic field.

For comparison, we have made another set of topographic and spectroscopic images taken at a much lower temperature (100 K). The results are shown in Fig. 3. As is evident from Fig. 3(b), the metallic region has occupied a much larger fraction at this temperature. Moreover, it shows an intimate correlation with the grain structure shown in a topographic image [Fig. 3(a)]. This is not surprising because as the sample becomes more magnetically ordered at lower temperatures, more metallic regions are expected to form. Furthermore, as shown in Fig. 3(c), the spectroscopic image taken at an applied magnetic field of 0.35 T is essentially the same as that obtained in zero field [Fig. 3(b)], indicating that the phase distribution is more stable and insensitive to exter-

nal perturbation at lower temperatures. In Fig. 3(d), the morphology and dI/dV curves scanned along the white lines in Figs. 3(a)–3(c) show an intimate correlation between the grain structure and the respective phases.

In $La_{1-x}Ca_xMnO_3$ $(0.2<x<0.5)$, it is generally believed that the MIT is governed by the hopping of electrons in e_g orbital between neighboring Mn^{3+} and Mn^{4+} sites with strong on-site Hund's coupling by an O^{2-} ion.[5] In the crossover regime around T_C, the transformation from disordered random spin into ordered ferromagnetic phase can occur only gradually. This, in turn, results in a state of coexisting multiphase. In this state, evidence has shown that the volume fraction of metallic phase could be modulated by either external electric field[14] or external magnetic field.[10] This naturally explains the current results. The fact, that not only the volume fraction but also the distribution of the respective phases are dependent on the history of applied magnetic field, is indicative of short-range magnetic ordering at temperatures not far below T_C. When the temperature is well below the transition temperature, the phase separation evolves to a more ordered and stable state.

Although our observations agree mostly with that reported by Fäth *et al.*,[10] some subtle differences are noted. Namely, the percolated metallic phase in $La_{1-x}Ca_xMnO_3$ thin films appears to be intimately correlated with the grain structure in this study, in contrast to the uncorrelated scenario suggested by Fäth *et al.*[10] In addition, the metallic regions observed in this study are within a few tens of nanometers. This length scale is about an order of magnitude smaller than that reported in Ref. 10. The discrepancy may be due to the temperature range and field strength studied in respective investigations. On the other hand, both results are in sharp contrast to the conclusions drawn by Grévin *et al.*,[11] in that the percolation paths are believed to follow electronically connected crystallites with ''better'' grain boundaries.

In summary, we have evidently observed the phase separation in $La_{0.67}Ca_{0.33}MnO_3$ thin films at temperatures below T_C. In particular, when the temperature is not far below T_C, the distribution of the percolated metallic paths can be susceptible to external fields. This is believed to arise from the short-range ordering in the crossover regime. Indeed, as the temperature is further lowered, the morphology of phase separation is much more robust and insensitive to external perturbations. The phase separation is also found to correlate closely with the underlying grain structure.

This work was supported by the National Science Council of Taiwan, ROC under Grant No. NSC90-2112-M-009-027.

[1] C. N. R. Rao, J. Phys. Chem. B **104**, 5877 (2000).
[2] C. Zener, Phys. Rev. **82**, 403 (1951).
[3] A. J. Millis, P. B. Littlewood, and B. I. Shraiman, Phys. Rev. Lett. **74**, 5144 (1995).
[4] R. Maezono, S. Ishihara, and N. Nagaosa, Phys. Rev. B **58**, 11583 (1998).
[5] For a review, see E. Dagotto, T. Hotta, and A. Moreo, Phys. Rep. **344**, 1 (2001), and references therein.
[6] J. Y. T. Wei, N.-C. Yeh, and R. P. Vasquez, Phys. Rev. Lett. **79**, 5150 (1997).
[7] R. Akiyama, H. Tanaka, T. Masumote, and T. Kawai, Appl. Phys. Lett. **79**, 4378 (2001).
[8] A. K. Kar, A. Dhar, S. K. Ray, B. K. Mathur, D. Bhattacharya, and K. L. Chopra, J. Phys.: Condens. Matter **10**, 10795 (1998).
[9] A. Biswas, S. Elizabeth, A. K. Raychaudhuri, and H. L. Bhat, Phys. Rev. B **59**, 5368 (1999).
[10] M. Fäth, S. Freisem, A. A. Menovsky, Y. Tomioka, J. Aarts, and J. A. Mydosh, Science **285**, 1540 (1999).
[11] B. Grévin, I. Maggio-Aprile, A. Bentzen, L. Ranno, A. Llobet, and Ø. Fischer, Phys. Rev. B **62**, 8596 (2000).
[12] K. Dörr, J. M. De Teresa, K. H. Müller, D. Eckert, T. Walter, E. Vlakhov, K. Nenkov, and L. Schultz, J. Phys.: Condens. Matter **12**, 7099 (2000).
[13] S. J. Liu, J. Y. Juang, K. H. Wu, T. M. Uen, and Y. S. Gou (unpublished).
[14] T. Wu, S. B. Ogale, J. E. Garrison, B. Nagaraj, A. Biswas, Z. Chen, R. L. Greene, R. Ramesh, and T. Venkatesan, Phys. Rev. Lett. **86**, 5998 (2001).